Theoretical study of the Si/GaAs(001)-$c(4\times4)$ surface

J. M. Bass* and C. C. Matthai
Department of Physics, University of Cardiff, P.O. Box 913, Cardiff CF2 3YB, United Kingdom
(Received 10 October 1996; revised manuscript received 16 January 1997)

The deposition of Si on the GaAs(001)-$c(4\times4)$ reconstructed surface is studied with the aid of *ab initio* pseudopotential calculations. With reference to the results of scanning tunneling microscopy (STM), reflectance anisotropy spectroscopy (RAS), and reflection high-energy electron diffraction experiments, models for the Si/GaAs(001)-$c(4\times4)$ surface are constructed with Si coverages corresponding to 0.25 and 1.0 ML. STM images are simulated and RAS spectra are calculated for these models and compared with experiment. By examining the local density of states and the magnitude of the optical transition matrix elements it is possible to make a link between the features in the RAS spectra and surface electronic structure. Comments are made on the validity of these surface structural models. [S0163-1829(97)06819-7]

I. INTRODUCTION

The study of the deposition of Si on the GaAs(001) surface is motivated not only by the need to understand the formation of semiconductor interfaces, but also, in this case, by the possibilities created through allowing the Si atoms to form a dopant layer in the bulk GaAs. Since it was first shown that, by momentarily interrupting the metal organic vapor phase epitaxial growth of GaAs and allowing the subsequent adsorption of Si on the growing surface, it was possible to produce a sharp doping spike,[1] interest has grown steadily in the concept and applications of δ doping.[2–4] Although many different combinations of δ dopants and semiconductors are possible, the majority of interest has centered around using Si and Be as δ dopants in GaAs and $Al_xGa_{1-x}As$. Such δ-dopant layers may, for example, be used to alter the band offsets at a semiconductor heterojunction[5,6] or to control the Schottky barrier height at a metal-semiconductor interface.[7] Possible device applications include nonalloyed Ohmic contacts, δ-doped doping superlattice lasers, and field-effect transistors.[2–4] To get the most from this technology it is necessary to be able to fabricate structures with δ-dopant layers of the highest possible quality. An understanding of the initial stages of formation of the dopant layer is therefore essential.

The scanning tunneling microscope (STM) is a well-established surface investigative tool which has been responsible for the conclusive determination of many surface structures. For example, in the case of the GaAs(001)-(2×4) reconstructed surfaces STM images[8] confirmed the concept of the missing dimer model.[9] Different phases for this surface were subsequently observed[10], labeled the α, β, and γ phases, and the STM eventually provided us with the generally accepted structural models for these surface phases, all of which have the basic feature of two As dimers per unit cell.[11,12] The route to this conclusion was not straightforward and indicated that, despite the obvious advantages of the STM, care is required in the interpretation of images. It would therefore be appropriate to use theoretical simulations as an aid to dismiss or support proposed surface structural models. Such simulations have been shown to be feasible,[13] and have been applied to a number of systems including GaAs(001)-reconstructed surfaces.[14]

The technique of reflectance anisotropy spectroscopy (RAS),[15] which measures the difference in reflectance for light of two orthogonal polarizations normally incident on a surface, is not as widely used as scanning tunneling microscopy (also STM), but is nevertheless a valuable tool in surface science. RAS has proved very useful in the study of GaAs(001)-reconstructed surfaces due to its sensitivity to the formation and destruction of surface dimers, which occur during epitaxial growth, and the fact that it can be used, *in situ*, in real time and in non-UHV conditions. Kamiya *et al.*[16] showed that the RAS spectral line shapes for the 2×4 and $c(4\times4)$ reconstructions are quite different from each other, making RAS an effective method for identifying them. As with STM there is also a need for calculations in order to fully exploit the power of RAS. Through calculations features in the RAS spectra may be assigned to specific optical transitions which can then be related to electronic or structural features of the surface.

We have previously demonstrated, using *ab initio* calculations, and considering one-electron optical transitions, that RAS spectra could be calculated which are directly comparable with experiment for the GaAs(001) reconstructed surfaces.[17] In particular it was demonstrated that the experimental spectra of the β phase of the 2×4 reconstructed surface could be interpreted as an admixture of the spectra of two different structural models for this surface, with the spectrum from the model which has two As dimers and Ga absent from the missing dimer trenches dominating, in agreement with the STM experiments. The calculated RAS spectra of the GaAs(001)-$c(4\times4)$ reconstructed surface was also found to agree with the experimental findings. Similarly Kipp *et al.*,[18] using the same computational approach, have recently shown that there is excellent agreement between the calculated and observed RAS spectra for the As/Si(001)-(2×1) reconstruction, which they initially characterized by STM. These results illustrate the reliability of RAS spectra obtained from the results of *ab initio* calculations.

Motivated by experimental work on the Si/GaAs(001)-$c(4\times4)$ reconstructed surface and the subsequent need to fully understand STM images and RAS spectra we have undertaken a theoretical study of this surface. STM images and

RAS spectra have therefore been calculated for models of the Si/GaAs(001)-$c(4\times4)$ surface corresponding to Si coverages of 0.25 and 1.0 ML in order to investigate structural, electronic and optical properties, and also to complement the experimental work. The energetics of these model surfaces are not studied, as we seek to compare them individually with experiment and not with each other. Moreover these models, as discussed in Sec. V, provide building blocks for larger, more complex, surfaces consisting of a variable number of dimers, so that a study of the surface energy is no longer straight forward. The remainder of this paper is arranged as follows. In Sec. II some of the experimental results on the Si/GaAs(001)-$c(4\times4)$ reconstructed surface are reviewed, and models for this surface are constructed using that information. The computational method used to simulate STM images and calculate RAS spectra is outlined in Sec. III. The results of these calculations are given in Sec. IV, where STM images, RAS spectra, and the local density of states are presented for each surface structural model. In Sec. V the validity of the models is discussed. Section VI concludes the paper.

II. MODELS FOR THE Si/GaAs(001)-$c(4\times4)$ SURFACE

The molecular-beam-epitaxial growth of the GaAs(001) surface normally takes place under As rich conditions. When the growth is terminated and the surface annealed under an As_4 flux, a 2×4 or $c(4\times4)$ reconstruction can be obtained depending on the As_4 pressure, the annealing time, and the temperature. Si can then be deposited under the continued presence of an As_4 flux. Although there have been a number of experimental studies of the deposition of Si on the GaAs(001)-(2×4) reconstructed surface,[19–23] we only concern ourselves here with the $c(4\times4)$ reconstruction. The generally accepted model for this reconstruction as deduced from STM images[24,11,12] and supported by x-ray-diffraction experiments[25] and total-energy calculations[26] is shown in unit cell (a) of Fig. 1. The surface is terminated with As, and then there are six extra As atoms per surface unit cell which form three As dimers orientated in the [110] direction so that the total As coverage is 1.75 ML.

Woolf *et al.*,[27] studied the deposition of Si on the GaAs(001)-$c(4\times4)$ surface using the techniques of RAS and reflection-high-energy electron diffraction (RHEED). Their RHEED results indicate that at a Si coverage of around 0.1 ML the surface begins to form a 1×2 reconstruction, which is fully developed by 0.15 ML and lasts up till 0.30 ML, at which point a 3×1 reconstruction begins to develop. For Si coverages greater than this and up to 1.0 ML only a 3×1 reconstruction is observed. They further found that the development of the RAS spectra, as a function of increasing Si coverage, also indicated a number of distinct phases for this surface. Additionally, it was observed that very low (0.01 ML) coverages of Si could be detected by the RAS spectrometer. The RHEED results of Avery *et al.*,[28] by contrast, indicate the initial formation of a 2×1 reconstruction at very low Si coverages, which then develops into an asymmetric 3×1 reconstruction at around 0.2 ML. The STM images, reported in the same work, show extended dimer rows orientated in the [110] direction at low Si coverages, and then at higher Si coverages dimer rows orientated in the [110] direction.

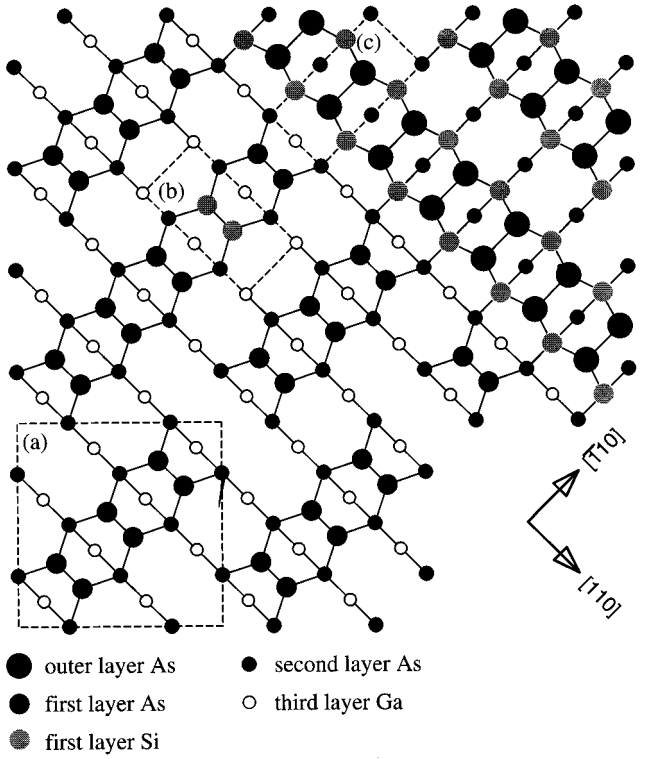

FIG. 1. Models for the GaAs(001)-$c(4\times4)$ reconstructed surface with the deposition of Si atoms.

These results suggest that it is possible to construct models for the Si/GaAs(001)-$c(4\times4)$ reconstructed surface using the following arguments. First, it is known that Si atoms occupy only Ga sites.[29] Second, although the first layer of each $c(4\times4)$ unit cell is covered with As atoms, the extra two unoccupied atom sites should still be thought of as Ga sites. Two Si atoms can then occupy these sites and form a dimer so that the surface then has a Si coverage corresponding to 0.25 ML. This is illustrated by unit cell (b) in Fig. 1. Strictly speaking, the surface still has $c(4\times4)$ periodicity, but if the Si dimers are regarded as being equivalent to the As dimers then the surface can be thought of as having a 1×2 periodicity consistent with the results of Woolf *et al.*[27] We shall refer to this $c(4\times4)$ unit cell, with two Si atoms, as model 1. To increase the Si coverage further, with the condition that the Si atoms must occupy Ga sites, then it is necessary for the Si atoms to perform a site exchange with the As atoms in the first layer. A site exchange mechanism using an As layer as a surfactant has theoretically been shown to be energetically favorable for the epitaxial growth of Ge on Si(001),[30] and Si on Si(001).[31] The displaced As atoms can then form an outer layer of dimer rows orientated in the [110] direction, as illustrated in unit cell (c) of Fig. 1. We shall refer to this model as model 2. The surface now has a 2×1 periodicity and a Si coverage of 1.0 ML. Although this is not the 3×1 periodicity, as observed by Woolf *et al.*[27] and Avery *et al.*,[28] a model with the required periodicity can simply be obtained by positioning the rows of As dimers one repeat distance further apart. These two models do, however, agree with the STM results of Avery *et al.* in that at low Si

coverages there are dimer rows orientated in the $[\bar{1}10]$ direction and then at higher Si coverages dimer rows orientated in the [110] direction.

III. COMPUTATIONAL TECHNIQUE

The starting point for both the simulation of STM images and the calculation of RAS spectra are the wave functions obtained from *ab initio* pseudopotential calculations. In brief, nonlocal pseudopotentials (optimized Kerker pseudopotentials[32]), the local-density approximation and the conjugate-gradient method were used to minimize the total energy through the relaxation of the electronic and atomic degrees of freedom.[33] The surface was represented by a supercell containing four layers of GaAs, a layer of hydrogen atoms terminating the bottom surface, and sufficient As and Si atoms on the top surface to create the required reconstruction. Sufficient layers of vacuum were then included to separate the two surfaces, making the total supercell thickness equivalent to eight layers of GaAs. Test calculations performed with both thicker and thinner GaAs slabs demonstrated that four layers of GaAs were adequate for calculating STM images and RAS spectra. Thicker GaAs slabs produced STM images and RAS spectra which were qualitatively no different to the ones presented in this paper. The top three layers of atoms were allowed to relax completely. The purpose of the hydrogen atoms is to remove the unwanted anisotropy from the bottom surface, which would contribute to the reflectance anisotropy of the supercell. A number of arrangements for the hydrogen atoms were investigated by calculating the RAS spectra of unreconstructed Ga-terminated slabs, and it was found that hydrogen atoms positioned directly below alternative Ga atoms produced nearly isotropic spectra. Charge transfer across the unit cell was not found to be a problem. It was also found that electronic states which were strongly located on the hydrogen atoms were close to the Fermi level, so optical transitions involving these states were largely in the region below 1 eV which is outside the range of interest. The four special k points $[(\frac{1}{8},\frac{1}{8},\frac{1}{4}), (\frac{1}{8},\frac{3}{8},\frac{1}{4}), (\frac{3}{8},\frac{1}{8},\frac{1}{4}), (\frac{3}{8},\frac{3}{8},\frac{1}{4})]$ used to perform the Brillouin-zone integration were also carefully chosen so as not to introduce any artificial anisotropy into the system. A basis set of plane waves was used which was cut off at an energy of 136 eV. This cutoff energy was found to reproduce the band gap of bulk GaAs through a cancellation of the underestimate of the band gap due to use of the local density approximation (LDA) and the effects of a smaller than ideal cutoff energy which causes the conduction-band states to shift upward. Test calculations did indeed reveal that, if the cutoff energy was increased, then the band gap would actually decrease down to the LDA value, and a ''scissors operator'' would then be necessary in order to compare calculated RAS spectra with experiment. The more serious problem, however, with using a low cutoff energy is that the description of the higher conduction-band states is less than reliable in terms of the relative ordering of the states and accuracy of the wave functions. Test calculations of the optical properties of bulk GaAs were performed, and the dielectric functions were found to agree well with experiment for energies up to $\sim$6 eV. Only at energies greater than this did the optical transition matrix elements became less dependable. In conclusion one may expect realistic values for the optical transition matrix elements and, more pertinently, the *difference* in the reflectance for two orthogonal polarizations to be reliable in the energy range of interest ($\sim$1–5 eV).

To generate STM images from the wave functions we go beyond the Tersoff s-wave approximation,[34] which is a statement of the fact that if the wave functions of the STM tip have spherical symmetry then the STM image will simply appear as the integrated local state density, $\int \rho(\boldsymbol{r},E)dE$, with the integral taken over filled or empty states within the vicinity of the Fermi level. Instead we used the Bardeen transfer Hamiltonian approximation,[35,13] a perturbative approach which allows the incorporation of realistic tip wave functions which in this work were obtained from a cluster of four Al atoms. Under the Bardeen formalism the tunneling current is given by

$$I(\boldsymbol{R},V_b)=\frac{2\pi e}{\hbar}\sum_{\mu\nu}|M_{\mu\nu}(\boldsymbol{R})|^2[f(E_\mu)-f(E_\nu)] \times\delta(E_\mu-E_\nu+eV_b),$$

where

$$M_{\mu\nu}(\boldsymbol{R})=\int \psi_\mu^*(\boldsymbol{r})(H-E_\nu)\psi_\nu(\boldsymbol{r}-\boldsymbol{R})d\boldsymbol{r}$$

are the tunneling matrix elements. $\psi_\mu(\boldsymbol{r})$ and $\psi_\nu(\boldsymbol{r})$ represent the surface and tip wave functions, respectively, $\boldsymbol{R}$ is the position of the tip relative to the surface, V_b is the tip-surface bias voltage, and $f(E)$ the Fermi distribution function. Because only a small cluster of atoms were used to represent the tip, the tip wave functions do not form a continuum as would be the case for a real tip so the δ function in the expression for the tunneling current was replaced by a Gaussian function,

$$\delta(E_\mu-E_\nu+eV_b)\rightarrow\frac{1}{\sigma\sqrt{2\pi}}\exp-\frac{1}{2}\left(\frac{E_\mu-E_\nu+eV_b}{\sigma}\right),$$

in order to smear out the discrete energy levels. A value of 1 eV was taken for σ which we previously found to reproduce reliably the scanning tunneling spectroscopy spectra for the GaAs(110) surface.[36]

To obtain the RAS spectra we performed two sets of calculations in parallel, one for light polarized along the [110] direction and the other for light polarized along the [110] direction. For each polarization the imaginary part of the dielectric function is calculated according to[37]

$$\varepsilon_2(\omega)=\frac{e^2\hbar^2}{\pi m^2\omega^2}\sum_{v,c}\int_{\mathrm{BZ}}|\langle\psi_{\mathbf{k}c}|-i\nabla_{\mathbf{r}}|\psi_{\mathbf{k}v}\rangle|^2 \times\delta(E_{\mathbf{k}c}-E_{\mathbf{k}v}-\hbar\omega)d\boldsymbol{k},$$

where $\psi_{\mathbf{k}v}$ and $\psi_{\mathbf{k}c}$ are, respectively, valence- and conduction-band states with energies $E_{\mathbf{k}v}$ and $E_{\mathbf{k}c}$. The real part of the dielectric function was then obtained from this via a Kramers-Kronig transform,

$$\varepsilon_1(\omega)=1+\frac{2}{\pi}\mathcal{P}\int_0^\infty\frac{\omega'\varepsilon_2(\omega')}{\omega'^2-\omega^2}d\omega'.$$

The dielectric function is related to the real and imaginary parts of the refractive index, n and k, respectively, through the relation

$$n+ik=\sqrt{\varepsilon_1+i\varepsilon_2}.$$

The reflectance is then given by

$$r=\frac{1-n-ik}{1+n+ik}.$$

We denote the calculated reflectance for each polarization direction as $r_{[\bar{1}10]}$ and $r_{[110]}$ respectively, so the reflectance anisotropy is defined as

$$\frac{\Delta r}{\overline{r}}=2\frac{r_{[\bar{1}10]}-r_{[110]}}{r_{[\bar{1}10]}+r_{[110]}}.$$

Only the real part of the reflectance anisotropy $\mathrm{Re}(\Delta r/\overline{r})$, as determined in experiment, is presented in Sec. IV.

IV. RESULTS

A. Scanning tunneling microscopy images

The simulated STM images presented in this section are all for negative tip-surface bias voltages such that occupied surface states are being probed. For the As-rich GaAs(001) and associated surfaces this is appropriate, as the dangling surface bonds are expected to be occupied. This will be discussed in more detail later in the context of electron counting theories. Images were also generated for positive tip-surface bias voltages, and it was found that not only was the magnitude of the tunneling current much reduced, but also that the resemblance to the actual surface structure was much less obvious. This is as expected, and ties in with difficulties reported by experimentalists in imaging these surfaces at positive bias voltages. All the STM images shown here plot the variation in the tunneling current for a constant tip-surface separation of 2 Å. Although this tip-surface separation is less than the generally accepted experimental values, tests with larger separations produced no significant qualitative differences in the images. Similarly, scans at constant current also failed to affect the simulated STM images in any significant way. For a fuller discussion of the differences between constant tip-surface separation scans and constant current scans, as well some examples of STM images of the GaAs(001) reconstructed surfaces at positive tip-surface bias voltages images, see Ref. 14.

The simulated STM image for the GaAs(001)-$c(4\times4)$ reconstructed surface, at a tip-surface bias voltage of -2 V, is shown in Fig. 2. This image shows the characteristic ''brickwork'' structure as seen in experimental images.[24,11,12] Each As atom in the surface layer is individually resolved indicating tunneling from occupied lone pair orbitals on the As atoms. The tunneling current from the central As dimer is less than that from the outer As dimers, despite the fact that the central As dimer is higher by 0.044 Å. This is consistent with high-resolution STM images. It was further found that at a lower bias voltage of -1 V the central As dimer was barely visible in the simulated STM images but at a higher bias voltage of -3 V the central As dimer acquired equal prominence to the outer As dimers.

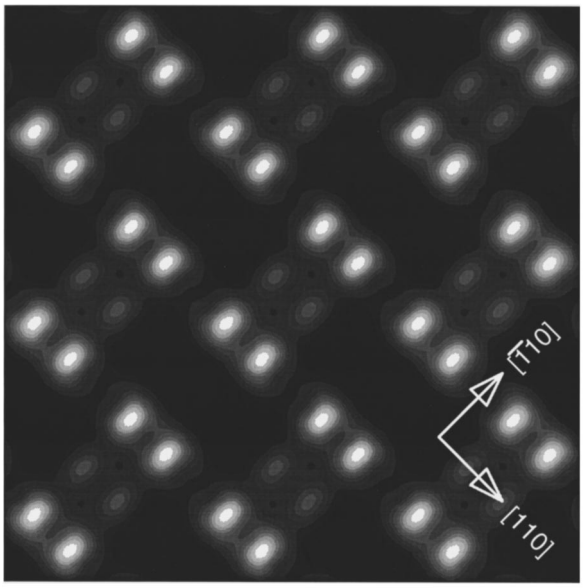

FIG. 2. Simulated STM image for the GaAs(001)-$c(4\times4)$ reconstructed surface at a bias voltage of -2 V.

Figure 3 shows the simulated STM image for model 1 at a tip-surface bias voltage of -1 V. The Si atoms in the surface layer can be seen in this image but not the As atoms. In the STM images shown in Fig. 4, where the bias voltage is -3 V, the As atoms in the surface layer are now visible, although there is a greater tunneling current emanating from the Si atoms. Overall the simulated STM image consists of rows of bright features orientated in the [110] direction, which can be thought of as an extension of the ''needlelike'' islands observed by Avery *et al.*[28]

Figure 5 shows the simulated STM image for model 2 at a tip-surface bias voltage of -3 V. Each As atom in the outer surface layer can be individually identified. The image therefore simply consists of the dimers rows of model 2

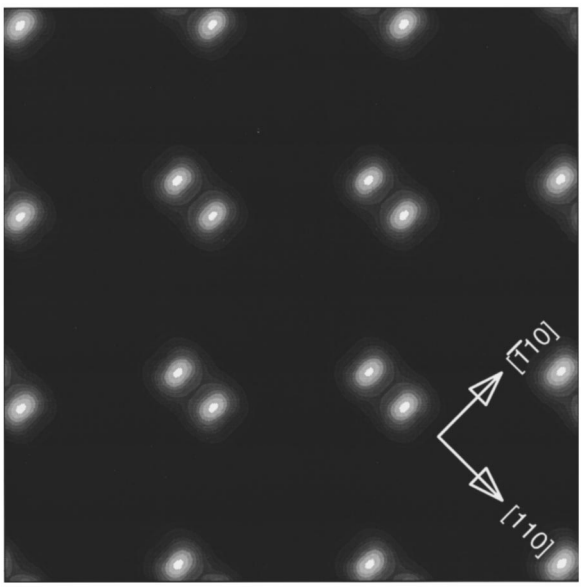

FIG. 3. Simulated STM image for model 1 at a bias voltage of -1 V.

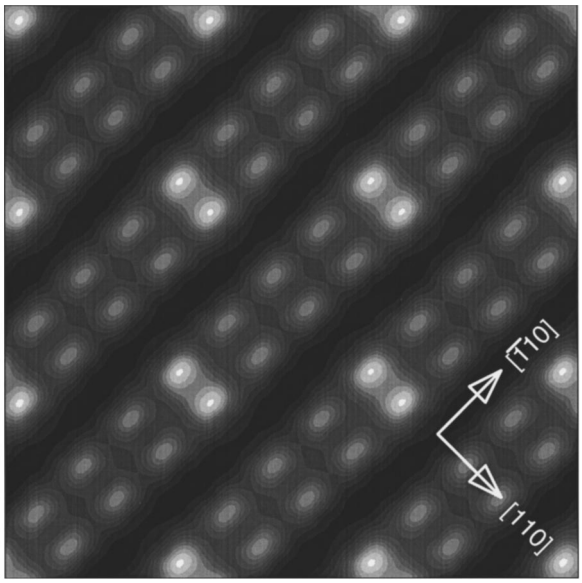

FIG. 4. Simulated STM image for model 1 at a bias voltage of −3 V.

which are orientated in the [110] direction. These can also be thought of as an extension of the ''needlelike'' islands observed by Avery *et al.*[28]

B. Reflectance anisotropy spectra

The calculated RAS spectra for the GaAs(001)-$c(4\times4)$ reconstructed surface and for the two models incorporating Si atoms are shown in Fig. 6. These are to be compared with the experimental RAS spectra for the corresponding Si coverages shown in Fig. 7. For the GaAs(001)-$c(4\times4)$ surface the agreement between theory and experiment is very good, with the calculations reproducing the characteristic dip in the spectra at ~2.7 eV. Similarly the calculated RAS spectrum for model 1 agrees well with the experimental spectrum of the GaAs surface at a Si coverage of 0.25 ML, reproducing

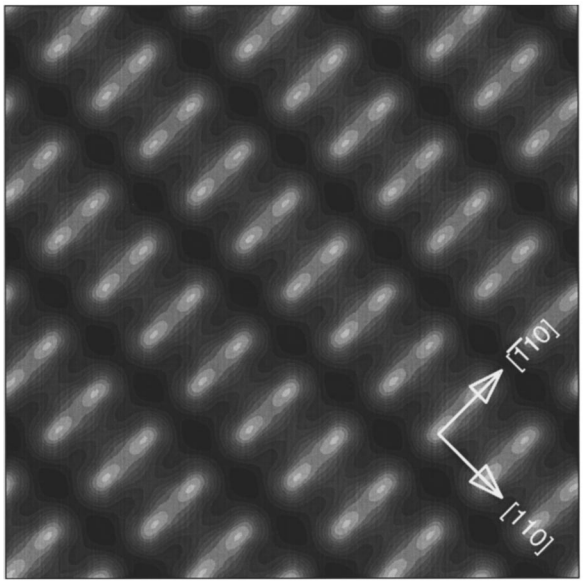

FIG. 5. Simulated STM image for model 2 at a bias voltage of −3 V.

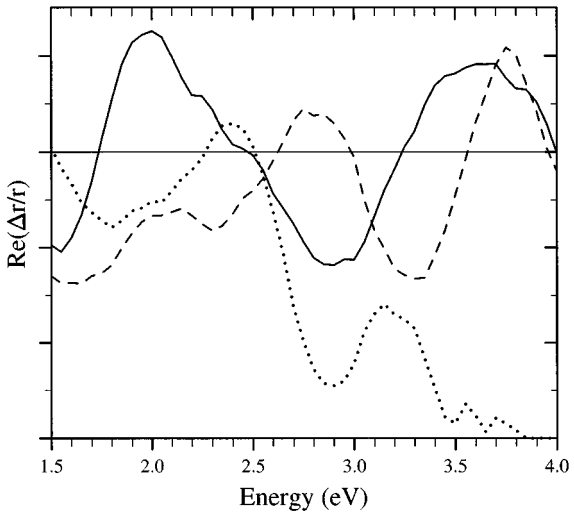

FIG. 6. Calculated RAS spectra for the GaAs(001)-$c(4\times4)$ reconstructed surface (solid line), for model 1 (dashed line) and model 2 (dotted line).

the peak at ~2.7 eV. However, for both of these calculated spectra the agreement with experiment is not so good at higher energies, where the principle features appear to have been shifted down in energy. This would seem to indicate problems with the energies of the higher conduction bands due to the use of density-functional theory, and also convergence problems caused by the termination of the plane-wave basis set used in the pseudopotential calculations. For model 2 the agreement between the calculated spectrum and the experimental spectrum of the GaAs surface at a Si coverage of 1.0 ML is poor although the sign of the reflectance anisotropy is correctly predicted. This poor agreement is in no doubt part due to the fact that the RHEED results of both Woolf *et al.*[27] and Avery *et al.*[28] report a 3×1 reconstruction for the surface at this Si coverage whereas model 2 only has a 2×1 periodicity.

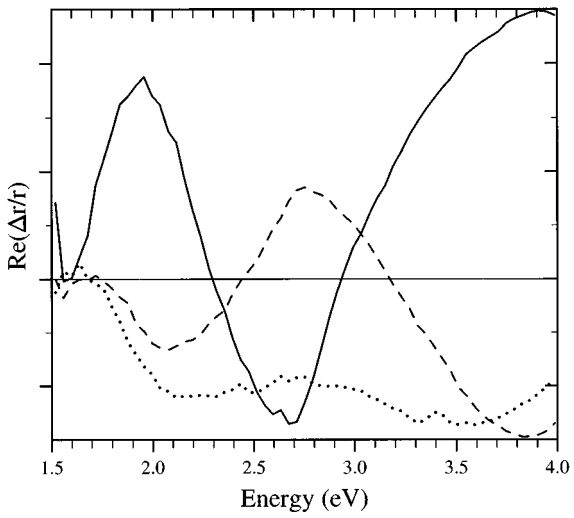

FIG. 7. Experimental RAS spectra for the GaAs(001)-$c(4\times4)$ reconstructed surface (solid line) and for Si coverages of 0.25 (dashed line) and 1.0 ML (dotted line) [taken from Woolf *et al.* (Ref. 27)].

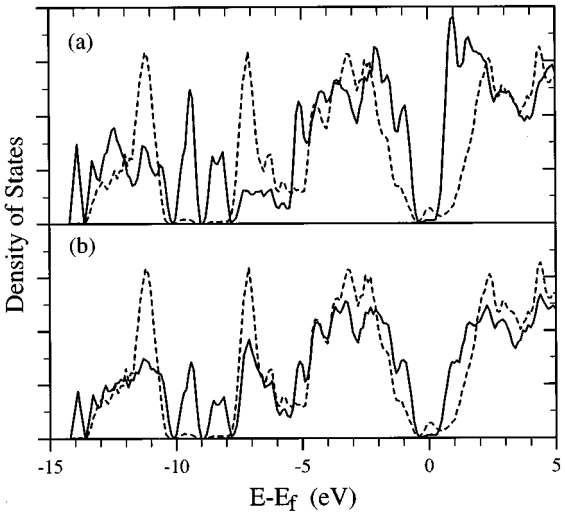

FIG. 8. LDOS for the GaAs(001)-$c(4\times4)$ reconstructed surface. (a) The surface layer of As atoms. (b) The GaAs layer below the surface. The dashed lines indicate the density of states for bulk GaAs taken from the central region of the slab.

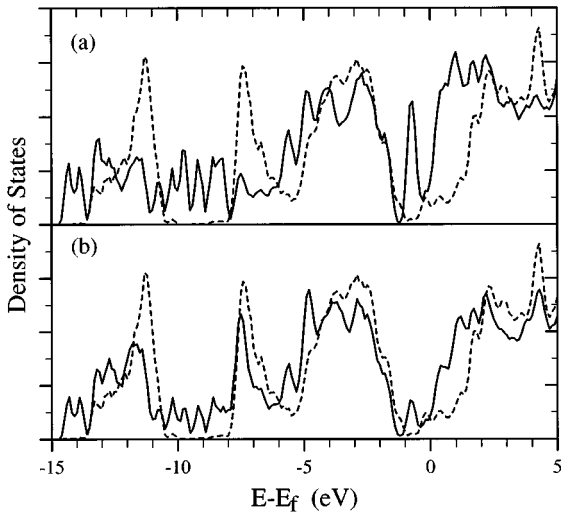

FIG. 9. LDOS for model 1. (a) The surface layer, which consists of six As atoms and two Si atoms per unit cell. (b) The GaAs layer below the surface. The dashed lines indicate the density of states for bulk GaAs taken from the central region of the slab.

C. Local density of states

An analysis of the local density of states (LDOS) is instructive in that it enables the identification of features in the surface electronic structure which can help explain the STM images. Moreover, if one observes that the RAS spectrum bears a close resemblance to the anisotropy of the surface dielectric function,[38,39] then features in the RAS spectrum can be linked to specific optical transitions. If this is done in conjunction with an examination of the LDOS, then it is possible to relate specific features in the RAS spectra to optical transitions which can then be linked to the surface electronic structure.

The LDOS for the GaAs(001)-$c(4\times4)$ reconstructed surface is shown in Fig. 8. There are distinct surface states at both the valence- and conduction-band edges which are associated with the surface layer of As atoms. The gradual emergence of the central As dimers in the STM images with increasing tip-surface bias voltage can be attributed to the three separate surface states in the valence band between 0 and -3 eV. The state closest to the Fermi level is localized on the outer As dimers, whereas the other two surface states are localized across all three As dimers. In examining which electronic states contribute to the dielectric function anisotropy and hence to the reflectance anisotropy, it was found that bulklike states in the valence band and surface states in the conduction band played a key role. The surface states in the valence band were found not to contribute significantly to the anisotropy of the surface dielectric function. This scenario is the same as we have previously reported for the GaAs(001)-(2×4) reconstructed surfaces.[17]

For model 1, an examination of the LDOS, shown in Fig. 9, indicates the presence of a pronounced surface state at ~1 eV below the Fermi level which was found to be strongly localized on the Si atoms in the surface layer. This explains why the Si atoms feature so prominently in the simulated STM images for this model at low bias voltages. Furthermore, it was found that this surface state contributed significantly to the dielectric function anisotropy, especially in vicinity of the feature at ~2.7 eV, explaining the sensitivity of the technique of RAS to very low Si coverages on the GaAs(001)-$c(4\times4)$ surface. The surface states in the conduction band continue to contribute to the dielectric function anisotropy.

The LDOS for model 2, shown in Fig. 10, indicates a surface state in the valence band localized on the outer As layer at ~2 eV below the Fermi level which is responsible for the rows of dimers seen in the STM images for this model. There are also surface states in the conduction-band which are associated with both the outer surface layer of As atoms and the layer of Si atoms below the surface. However the conduction-band surface states localized on the Si layer do not contribute significantly to the dielectric function anisotropy. In common with the other As-rich GaAs(001) re-

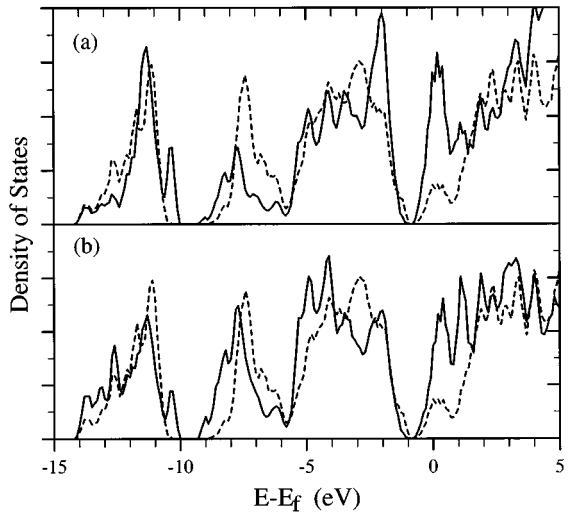

FIG. 10. LDOS for model 2. (a) The outer surface layer of As atoms. (b) The layer of Si atoms below the surface. The dashed lines indicate the density of states for bulk GaAs taken from the central region of the slab.

constructed surfaces, it was found that optical transitions between bulklike valence-band states and surface states in the conduction band were primarily responsible for the dielectric function anisotropy.

V. DISCUSSION

It goes without saying that the models proposed in this work for the Si/GaAs(001)-$c(4\times4)$ surface are highly idealized. The periodicity imposed by using a supercell reciprocal space technique ensure that these idealized surface models, are perfectly repeated to infinity. This clearly is not physical, and even the best-prepared surfaces will suffer from the effects of impurities, dislocations, steps, kinking in the dimer rows, and other imperfections, all of which serve to reduce the surface energy. It is necessary to bear this in mind when commenting on the validity of these models especially with regard to heuristic arguments such as the electron counting principle. The electron counting principle[9] or the octet rule,[40] when applied to the GaAs(001) surface, demands that to minimize the surface energy all As dangling bonds must be filled and all Ga dangling bonds emptied. The model used here for the GaAs(001)-$c(4\times4)$ reconstructed surface satisfies this rule. If the Si dangling bonds are taken to be occupied by virtue of their energy with respect to Fermi level, then model 1 has two surplus electrons per unit cell and does not satisfy electron counting. However, if a second As dimer is replaced with a Si dimer then there are two less electrons per unit cell and electron counting is satisfied. The number of electrons can be lowered further by either replacing more As atoms with Si or by completely removing As or Si dimers. Doing this, it will then be possible to obtain rows of dimers orientated in the $[\bar{1}10]$ direction consisting of either As or Si atoms and of arbitrary length. The same arguments can also be applied to model 2. This illustrates how by reviewing our idealized models in the light of simple arguments it is possible to reconcile them much more closely with more realistic surfaces such as those seen in the STM images of Avery *et al.*[28]

Because RAS is not a diffraction technique then simple sum-rule-type arguments can be applied to a surface consisting of several different domains of reconstructions. The measured RAS spectrum is expected to be that of the dominant reconstruction. So, although a real surface does not have perfect infinite rows of dimers, as long as such dimers are dominant then a calculated RAS spectrum for an idealized surface can still be reasonably compared to a experimental spectrum.

VI. CONCLUSION

With reference to the results of STM, RAS, and RHEED, we constructed models for the Si/GaAs(001)-$c(4\times4)$ reconstructed surface with Si coverages corresponding to 0.25 and 1.0 ML. STM images and RAS spectra were then calculated for these models and compared with experiment. The calculated RAS spectrum for model 1 was found to be in good agreement with the experimental spectrum suggesting that this model is representative of the surface structure. The additional agreement of the simulated STM images with experiment gives weight to this view. Based on this model we have therefore demonstrated that the sensitivity of the RAS spectral feature at $\sim$2.7 eV, with increasing Si coverage between 0 and 0.25 ML, is to be attributed to the presence of Si dimers on the surface. This is opposed to the view that it is the orientation of the As dimers that solely govern this feature. Finally, for higher Si coverages, the calculated RAS spectrum and STM images suggest that the Si atoms can form a layer underneath the top As layer. Hence RAS could be used as a means of monitoring the compactness of a Si layer.

ACKNOWLEDGMENTS

This work was supported by the Engineering and Physical Sciences Research Council (EPSRC), UK. The EPSRC is also acknowledged for the provision of resources on the Intel iPSC/860 supercomputer at the Daresbury Laboratory.

*Electronic address: bass@cf.ac.uk

[1] S. J. Bass, J. Cryst. Growth **47**, 613 (1979).
[2] K. Ploog, M. Hauser, and A. Fischer, Appl. Phys. A **45**, 233 (1988).
[3] E. F. Schubert, J. Vac. Sci. Technol. A **8**, 2980 (1990).
[4] J. J. Harris, J. Mater. Sci. Mater. Electron. **4**, 93 (1993).
[5] M. Peressi, S. Baroni, R. Resta, and A. Baldereschi, Phys. Rev. B **43**, 7347 (1991).
[6] L. Sorba, G. Bratina, A. Antonini, A. Franciosi, L. Tapfer, A. Migliori, and P. Merli, Phys. Rev. B **46**, 6834 (1992).
[7] T.-H. Shen, M. Elliot, R. H. Williams, D. A. Woolf, D. I. Westwood, and A. C. Ford, Appl. Surf. Sci. **56-58**, 749 (1992).
[8] M. D. Pashley, K. W. Haberern, W. Friday, J. M. Woodall, and P. D. Kirchner, Phys. Rev. Lett. **60**, 2176 (1988).
[9] D. J. Chadi, J. Vac. Sci. Technol. A **5**, 834 (1987).
[10] H. H. Farrell and C. J. Palmstrøm, J. Vac. Sci. Technol. B **8**, 903 (1990).
[11] Tomihiro Hashizume, Q.-K. Xue, A. Ichimiya, and T. Sakurai, Phys. Rev. B **51**, 4200 (1995).
[12] A. R. Avery, D. M. Holmes, J. Sudijono, T. S. Jones, and B. A. Joyce, Surf. Sci. **323**, 91 (1995).
[13] Masaru Tsukada, Katsuyoshi Kobayashi, Nobuyuki Isshiki, and Hiroyuki Kageshima, Surf. Sci. Rep. **13**, 265 (1991).
[14] J. M. Bass and C. C. Matthai, Phys. Rev. B **50**, 11 211 (1994); J. M. Bass, S. J. Morris, and C. C. Matthai, Mater. Sci. Eng. B **37**, 89 (1996).
[15] D. E. Aspnes and A. A. Studna, Phys. Rev. Lett. **54**, 1956 (1985).
[16] Itaru Kamiya, D. E. Aspnes, L. T. Florez, and J. P. Harbison, Phys. Rev. B **46**, 15 894 (1992).
[17] S. J. Morris, J. M. Bass, and C. C. Matthai, Phys. Rev. B **52**, 16 739 (1995); J. M. Bass and C. C. Matthai, J. Vac. Sci. Technol. B **14**, 3075 (1996).
[18] Lutz Kipp, D. K. Biegelsen, J. E. Northrup, L.-E. Swartz, and R. D. Bringans, Phys. Rev. Lett. **76**, 2810 (1996).
[19] L. Sorba, G. Bratina, G. Ceccone, A. Antonini, J. F. Walker, M. Micovici, and A. Franciosi, Phys. Rev. B **43**, 2450 (1991).
[20] K. Adomi, S. Strite, H. Morkoç, Y. Nakamura, and N. Otsuka, J. Appl. Phys. **69**, 220 (1991).
[21] H. J. Gillespie, G. E. Crook, and R. J. Matyi, Appl. Phys. Lett. **60**, 721 (1992).

[22] M. Wassermeier, J. Behrend, L. Däweritz, and K. Ploog, Phys. Rev. B **52**, R2269 (1995).
[23] A. R. Avery, J. L. Sudijono, T. S. Jones, and B. A. Joyce, Surf. Sci. **340**, 57 (1995).
[24] D. K. Biegelsen, R. D. Bringans, J. E. Northrup, and L.-E. Swartz, Phys. Rev. B **41**, 5701 (1990).
[25] M. Sauvage-Simkin, R. Pinchaux, J. Massies, P. Calverie, N. Jedrecy, J. Bonnet, and I. K. Robinson, Phys. Rev. Lett. **62**, 563 (1989).
[26] John E. Northrup and Sverre Froyen, Phys. Rev. Lett. **71**, 2276 (1993).
[27] D. A. Woolf, K. C. Rose, J. Rumberg, D. I. Westwood, F. Reinhardt, S. J. Morris, W. Richter, and R. H. Williams, Phys. Rev. B **51**, 4691 (1995).
[28] A. R. Avery, J. Sudijono, D. M. Holmes, T. S. Jones, and B. A. Joyce, Appl. Phys. Lett. **66**, 3200 (1995); A. R. Avery, D. M. Holmes, J. Sudijono, T. S. Jones, M. R. Fahy, and B. A. Joyce, J. Cryst. Growth **150**, 202 (1995).
[29] L. Hart, M. R. Fahy, R. C. Newman, and P. F. Fewster, Appl. Phys. Lett. **62**, 2218 (1993).
[30] Byung Deok Yu and Atsushi Oshiyama, Phys. Rev. Lett. **72**, 3190 (1994).
[31] Takahisa Ohno, Phys. Rev. Lett. **73**, 460 (1994).
[32] G. P. Kerker, J. Phys. C **13**, L189 (1980).
[33] M. C. Payne, M. P. Teter, D. C. Allan, T. A. Arias, and J. D. Joannopoulos, Rev. Mod. Phys. **64**, 1045 (1992).
[34] J. Tersoff and D. R. Hamann, Phys. Rev. Lett. **50**, 1998 (1983).
[35] J. Bardeen, Phys. Rev. Lett. **6**, 57 (1961).
[36] J. M. Bass and C. C. Matthai, Phys. Rev. B **52**, 4712 (1994).
[37] H. Ehrenreich and H. R. Phillips, Phys. Rev. **128**, 1662 (1962).
[38] H. T. Anyele, T.-H. Shen, and C. C. Matthai, J. Phys. Condens. Matter **8**, 4139 (1996).
[39] D. E. Aspnes, L. T. Florez, A. A. Studna, and J. P. Harbison, J. Vac. Sci. Technol. B **8**, 936, (1990).
[40] S. B. Zhang and Alex Zunger, Phys. Rev. B **53**, 1343 (1996).